

Detecting Grasping Sites in a Martian Lava Tube: Multi-Stage Perception Trade Study for ReachBot

Julia Di
Dept. of Mech. Engineering
Stanford University
Stanford, CA 94305
juliadi@stanford.edu

Abstract—This paper presents a trade study analysis to design and evaluate the perception system architecture for ReachBot. ReachBot is a novel robotic concept that uses grippers at the end of deployable booms for navigation of rough terrain such as walls of caves and lava tubes. Previous studies on ReachBot have discussed the overall robot design, placement and number of deployable booms, and gripper mechanism design; however, analysis of the perception and sensing system remains underdeveloped. Because ReachBot can extend and interact with terrain over long distances on the order of several meters, a robust perception and sensing strategy is crucial to identify grasping locations and enable fully autonomous operation. This trade study focuses on developing the perception trade space and realizing such perception capabilities for a physical prototype. This work includes analysis of: (1) multiple-range sensing strategies for ReachBot, (2) sensor technologies for subsurface climbing robotics, (3) criteria for sensor evaluation, (4) positions and modalities of sensors on ReachBot, and (5) map representations of grasping locations. From our analysis, we identify the overall perception strategy and hardware configuration for a fully-instrumented case study mission to a Martian lava tube, and identify specific sensors for a hardware prototype. The final result of our trade study is a system design conducive to benchtop testing and prototype hardware development.

TABLE OF CONTENTS

1. INTRODUCTION.....	1
2. BACKGROUND	2
3. SYSTEM TRADE STUDY PROCESS.....	3
4. PERCEPTION SENSOR SELECTION.....	4
5. SENSOR TRADE RESULTS	6
6. GRASPING SITE REPRESENTATION ANALYSIS	8
7. CONCLUSIONS.....	8
APPENDICES.....	9
A. MODALITY ANALYSIS	9
B. SENSOR ANALYSIS	9
ACKNOWLEDGMENTS	11
REFERENCES	11
BIOGRAPHY	12

1. INTRODUCTION

Skylights and caves on Mars and the Moon could yield astrobiological samples, unlock answers for geological origins, and reveal a previously undiscovered subsurface world. While there is clear scientific value in such environments, exploring them is a daunting technical challenge: navigating perilous, unknown terrain requires an innovative solution capable of versatile mobility through loose material and

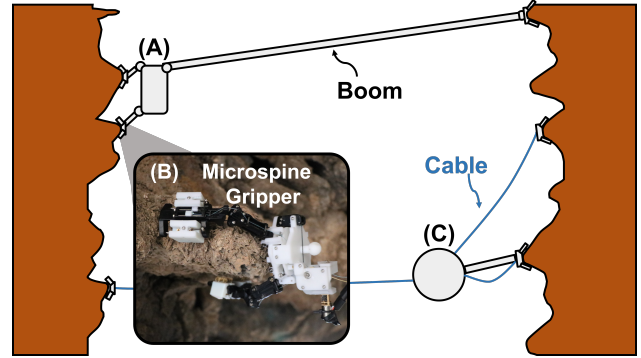


Figure 1. A diagram illustrating different ReachBot configuration concepts for a martian lava tube mission. (A) shows a ReachBot configuration concept using extendable booms. An eight-boom configuration has been explored in previous work. At the end of each boom is a microspine gripper that can grasp onto rough surfaces. (B) is an image of a ReachBot microspine gripper previously tested on lava tube rocks. (C) shows a ReachBot configuration that combines cables with booms for placing the grippers.

unpredictable obstacles. ReachBot is a robot concept that answers this call for mobility in extreme environments.

As discussed in previous work [1–5], ReachBot’s limbs are extendable booms that act as prismatic joints to achieve a large workspace compared to traditional rigid-link designs. These steerable booms, when paired with grippers, enable ReachBot to climb and span steep verticals inside caverns that a jumping robot or aerial robot may fail to access, as shown in Fig. 1(A,B). Furthermore, the booms could also be combined with other technologies, such as cables or tethers as shown in Fig. 1(C), to further increase reach and reduce mass and volume complexity. ReachBot’s large workspace expands the number of reachable anchor points in the environment, which is especially advantageous in unknown environments with sparse anchor points or obstructions in terrain.

To grasp the environment, the gripper at the end of each boom is equipped with microspines. Microspines have been used in multiple works to grasp rough and rocky surfaces, including for planetary exploration [6–10], and several works have analyzed the conditions for successful grasping with microspines [8, 11, 12]. As shown in Fig. 1(B), the ReachBot gripper successfully grasps surface locations that are approximately convex.

While ReachBot’s mechanical architecture and motion planning have been extensively studied, analysis of the perception system trade space has been comparatively scant. Early work

indoors assumed known grasping locations as captured by overhead cameras [2]. Later, a two-stage perception strategy and sensor system was introduced in a successful field testing demonstration in a Mojave Desert lava tube [13], but this only used RGB-D images in daylight and did not review other sensing modalities or mission-level considerations. Although RGB-D images work in the field, alternatives should be investigated for more realistic mission conditions. To operate in caves and skylights, every perception system faces the typical subsurface concerns—low power, limited communication bandwidth, total darkness, and dusty conditions. These are in addition to and compounded by the operational challenges of any space hardware—radiation hardening, thermal requirements, mass/volume restrictions, cost, and technological risk. Because ReachBot has a much larger workspace than that of a typical climbing robot, examination of high-level sensing strategies is also warranted.

Statement of Contributions—This work evaluates perception system approaches that enable ReachBot to identify grasping sites, building upon previous ReachBot analysis as well as existing work for subsurface robots that use distance-based sensing. The main contributions of this work are:

- We present a survey of different robotic sensing modalities for a climbing robot in a subsurface environment.
- We discuss perception system strategies and candidate map outputs of a ReachBot perception system
- We propose evaluation criteria of sensor hardware for a configuration of ReachBot that discerns grasping locations in a martian lava tube environment.
- We conduct trades and propose a hardware configuration that could be physically prototyped for testing in a lava tube environment.

Paper Organization—The rest of this paper is organized as follows. Section 2 describes background literature on the perception systems of robots designed for either climbing with microspines or subsurface exploration. We also discuss considerations for upstream trades around choice of perception strategy, and downstream trades on choice of environment representation for the planner. Section 3 discusses the trade study process. Then we develop evaluation criteria for sensor selection in Section 4 and present the viable perception architectures in Section 5 for a specific ReachBot mission. We follow with analysis of the different map representation choices in Section 6. Finally, we provide conclusions and suggest next steps for this work.

2. BACKGROUND

Perception Considerations for Microspine Robots

Others have built robotic systems using microspines for climbing. Most notably, LEMUR 3 from JPL is a multi-limbed robot that was field tested in a lava tube environment; their perception system was an actuated LiDAR system on the body to construct a map of grasping locations [7, 14]. We note however that LEMUR and its variants are all climbing robots that hug the rock wall, enabling body-mounted sensors to return highly dense and informative geometric reconstructions. ReachBot meanwhile climbs by pulling on the environment with potentially extra-long limbs. A body-mounted sensor on ReachBot will almost always return much sparser data compared to a more traditional climbing robot due to the increased distance from the rock walls. Therefore, designing the perception system for ReachBot requires more attention to criteria involving scene reconstruction from afar.

Perception for Exploration in Subterranean Environments

Perception systems for autonomous navigation in confined and subterranean spaces have been carefully evaluated, most recently with the DARPA Subterranean Challenge, which involved teams of robots searching for and detecting artifacts placed in an unknown subterranean environment [15]. There are a number of relevant surveys and challenge retrospectives [16–20] that discuss in further detail the learnings from this Challenge.

Of import is that the majority of teams used a combination of LiDAR and IMU as the primary sensing component. LiDAR units return accurate long-range depth measurements and are illumination invariant; IMUs are not sensitive to environmental disturbances and help distinguish between places with the same perceptual appearance [16]. Various other types of sensing (e.g. vision, thermal, odometry) is used in addition to LiDAR to increase redundancy especially when there are adverse conditions [18]. Multimodal perception, especially that combining LiDAR with another modality, continues to be investigated for subsurface robotics [21, 22]. Many teams also designed the perception system payload to be modular, allowing for standardized calibration and decoupling the system from other hardware.

ReachBot Perception Strategy Considerations

The perception system must generate a map of grasping sites for the planner. Because booms lose pointing accuracy when extended long distances, making the correction of large positional errors cumbersome, a two-stage strategy has been proposed [13]. This involves a single RGB-D camera mounted on a boom, which first perceived regions of interest from afar (boom in a stowed position), and then finalized the grasping site locations when the boom deploys closer to the surface. Here, we discuss the perception strategies for ReachBot more generally.

A one-stage perception process involves a perception sensor suite only mounted on the main body of ReachBot. We assume the use of multiple sensors in this sensor suite because the body of ReachBot can hold more mass than the booms, and multiple sensors reduce the risk that ReachBot cannot perceive its surroundings. However, for ReachBots with multiple long-range booms that can extend dozens of meters in large-diameter lava tubes, the aforementioned pointing accuracy becomes an issue. It follows that a one-stage perception process is better suited for a ReachBot configuration with short booms for a narrow space such as a slim vent. In other words, one-stage perception process allows for only far-field sensing, and perceived spatial resolution (thus accuracy) does not scale with boom length.

A two-stage perception process of both far-field and near-field sensing has the benefit of additional sampling, which increases accuracy in grasping site predictions. This process does pose an additional requirement: either having a lightweight sensor mounted on the distal end of the boom to enable near-range sampling (in addition to or in place of a body sensor), or a motion planning procedure to bring a body-mounted sensor closer to the desired surface. Implementation of the former for multiple booms depends on the permissible mass budget of the boom and the scale of distances covered. The latter could be accomplished with more stringent stance planning, or with hybrid locomotion schemas such as rolling and climbing.

A related question is whether there should be any gripper-

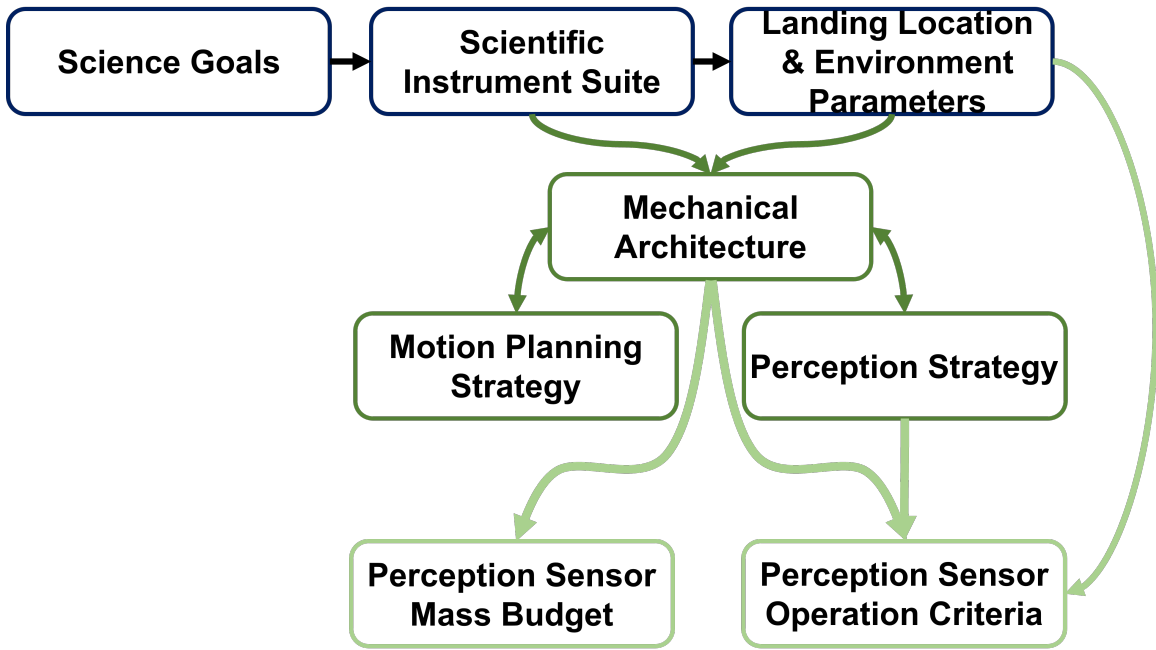


Figure 2. A flowchart depicting the trade study process in this work detailed in Section 3, which begins with the dictation of Science Goals for the mission. Initial engineering trades (dark green) are derived from science parameters, with perception requirements (light green) further derived downstream.

level sensing, for perceiving contact. One may then implement all three scales of sensing: far-field, near-field, and gripper-based sensing (or a subset). Instrumenting microspine grippers with force-torque, proximity, or tactile sensing could yield a number of benefits. A benefit is that estimating distance of the gripper to the surface could be used in a feedback loop to trigger the grasping sequence onto a surface (in previous tests, grasping sequences were always triggered manually). Force-torque information at the wrist could also be used for detecting gripper contact and monitoring grasping events. Sensor choice on the distal end must trade against the permissible mass budget of the boom.

3. SYSTEM TRADE STUDY PROCESS

The objective of this trade study is to determine the set of perception sensing modalities for ReachBot. We take inspiration from space engineering trade study methodologies [23] to establish the following architectural configuration variables traced from the science mission objectives, as shown in the flowchart of Fig. 2. These variables are not exhaustive, but we use them to make initial trade decisions to narrow the space, which are summarized in Table 1.

Science Goals

All technical specifications, including the perception strategy and sensor choices, should be in support of a clear scientific mission. Previous work has studied and proposed several potential top-level science missions for ReachBot [24] based on the key questions highlighted in the most recent Planetary Decadal Survey [25]. We summarize the missions below:

- Layered stratigraphy measurements of escarpments in the Polar Layered Deposits (PLDs) of Mars
- Layered stratigraphy measurements along volcanic cliffs.
- Exploration of subsurface conditions in lava tubes or caves

The perception system design depends on the specific environment selected. For example, a polar region expedition will have to account for potentially highly specular icy walls, and need ground testing of sensors in these expected conditions. For this work, we focus on the lava tube and cave exploration mission, which is detailed in [24] and builds upon the existing mechanical and motion planning system design analyzed in [3]. As a result of this mission choice, we anticipate perception system trades on operation in poor illumination and operation in dusty conditions.

Instrument Suite

Furthermore, the set of measurements defined in the Science Traceability Matrix from [24] dictate the instrument and sensor suite. The selected scientific instruments include complementery spectrometers and a radiation detector, which have a 25% margined mass of 15.1 kg. We note that any additional sensors such as optical cameras could have a dual scientific and engineering use. For example, visible spectrum or Light detection and ranging (LiDAR) data used for mapping could also be used to determine geological features. Scientific instruments are located on the main body of the robot and we do not consider alternatives in this work.

Terrain Parameters

Because martian lava tubes and caves have not been explored before, and because the subsurface precludes satellite pre-mapping, we assume the terrain to be uneven and unknown. Previous work has already described different terrain topologies that ReachBot concept may encounter on a mission [3]. We briefly list them here:

- ReachBot spanning a corridor, where the cavity is smaller than the span of the robot.
- ReachBot against a wall, which is mostly vertical or overhanging.
- ReachBot against the floor, where non-zero gravity is push-

ing the robot to the ground.

The perception system must perform well in all three expected terrain topology conditions. Based on previous surveys on Mars, we assign the dimensions of a representative lava tube as 30 m depth, and 300 m width based on average estimates [26]. Because lava tubes and caves on Mars have not yet been explored, we do not have measurements for the expected density of anchor points. Towards building a physical ReachBot prototype, we assume the existence of some anchor points in a test environment, though the spatial frequency of these points may be irregular.

ReachBot Configuration

As depicted in Fig. 1, one may envision several ReachBot concepts that make use of extendable booms capped with microspine grippers. We would like the following perception system analysis to be largely agnostic to the details of the specific ReachBot carrier robot. The only strict assumption we make is that all considered ReachBot concepts will have a central body and at least one extendable boom for placing microspine grippers onto the surface. This allows for both the body and the distal end of the boom as perception sensor placement possibilities. The central body may take any form, and booms may extend up to tens of meters [27].

However, in order to provide a mass budget for the sensor suite, we do assume a ≈ 10 m boom extension length and build from previous work on an eight-boom ReachBot configuration.

ReachBot Mass Budget

The mass budget of the central body and distal end of the boom will dictate what sensors may be placed there (if at all). In the following calculations, we assume any wiring masses to be trivial.

Previous work had assigned a mass budget of 10 kg [3] for an eight-boom prototype, but had assumed booms of trivial mass; and 30 kg had been assigned in even earlier work [1]. For a more detailed description of the mass budget, we look towards existing characterization of long, lightweight deployable booms. Fourteen-meter deployable booms for space sails have previously been tested and assigned a mass density of 62 g per meter [27]. With this construction, a 10 m-long ReachBot boom would yield a 0.62 kg total mass which scales linearly with the number of booms. For example, the eight-boom configuration introduced previously yields ≈ 5 kg across all booms.

With a conservative estimate of ≈ 22.5 N pulloff force per gripper [13] and in Mars gravity conditions, we expect to be capable of carrying the 10 to 30 kg mass budget range assigned previously. Assuming a 30 kg budget, given 5 kg for eight booms and a margined mass of 15.1 kg for the required scientific sensor suite, we will assign 20% of the remainder or ≈ 2 kg for the perception sensors located on the body. We note that the eight-boom design is likely the upper threshold on number of booms (designed to achieve force closure), and that there are other configurations with fewer booms (and therefore reducing mass).

A mass budget for the distal end of the boom can also be derived. Specifically, the limiting case for boom failure is buckling [3]. The most buckling load is experienced when the boom is completely outstretched and perpendicular to the direction of gravity. In this configuration, the boom supports

the weight of the boom, the weight of the gripper, and the weight of any sensor(s) at the distal end as given by:

$$M_{\text{shoulder}} = (m_{\text{sensor}} + m_{\text{gripper}} + \frac{1}{2}m_{\text{boom}})g_{\text{Mars}}L \quad (1)$$

where M is the buckling moment felt at the shoulder, m is mass, $g_{\text{Mars}} = 3.71 \text{ ms}^{-2}$, and $L = 10$ meters. A critical buckling moment of $M = 59.8 \text{ N m}$ was reported in for the 14-meter deployable space sail boom [27, 28]. Applying a 25% margin on the buckling moment, and using $m_{\text{boom}} = 0.62 \text{ kg}$ and $m_{\text{gripper}} = 0.25 \text{ kg}$ (gripper mass reported in [13]), we find that the sensor(s) may have a mass up to 0.72 kg when located at the distal end of the boom.

ReachBot Perception Strategy

As analysed in Section 2, a two-stage perception process has the benefit of additional sampling, and is preferred over a one-stage perception process especially when ReachBot is in an environment with potentially wide expanses to cover. Based on the mass budget analysis, we are able to accommodate sensing at the body and at the distal end of the boom, thus allowing for a two-stage perception strategy. We leave open the possibility of force sensing at the gripper and defer the specifics to future work.

We define the "near-field" distance as one-third of the length of the boom; for example, for a 10-meter boom, the range for near-field sensing is 3.3 m or closer to the surface.

As part of the trade study process, we will investigate the benefits and drawbacks of different sensor modalities.

4. PERCEPTION SENSOR SELECTION

To avoid the time and cost of sensor development, this perception system trade study is interested in analysing only commercial-off-the-shelf (COTS) or mature laboratory technology for a ReachBot concept prototype. Because we aim to prototype this in a full ReachBot system, we also do not consider highly expensive sensors in this survey. In some cases, modifications to sensors are proposed to increase performance or range for comparison. In the following, we summarize common range-sensing technologies and provide a list of criteria for evaluation for a ReachBot perception system.

Range-Sensing Technologies for Subsurface

Unlike wheeled or quadruped robots, which interact mostly with the ground floor, ReachBot and other such climbing robots will have significantly more interaction with the walls and ceilings of an environment. Several works have studied and compared perception sensor categories for subterranean robotics [20, 30, 31], though to our knowledge this is the first such analysis for a subsurface robot with a multiple-stage perception strategy. In this work, we consider the following range-sensing technologies: LiDAR, 2D cameras (monocular), 3D cameras (RGB-D or Time of Flight (ToF)), sonar, radar, and thermal.

LiDAR—LiDAR sensors are commonly used in robotics for mapping the environment. LiDAR sensors measure ToF of short laser pulses. These pulses can be rastered using spinning mirrors to generate a point cloud of the surroundings. More specifically, the ToF data is dependent on and thus

Table 1. We make architectural trades to narrow the trade space, as summarized in this table.

Trade Space Variable	Selected Definition
Environment Location	Lava tube or cave within the Arsia North region of Mars [29]
Terrain Parameters	Lava tube or cave up to 30 m depth and 300 m width.
Instrument Suite Location	Science instruments are only on the ReachBot body.
ReachBot Configuration	Concept includes one central body and at least one extending boom that may place microspine grippers onto a grasping location. Booms extend 10 m. Wiring mass trivial.
ReachBot Mass Budget	Up to 2 kg body-based sensor(s), 0.72 kg gripper-based sensor(s) with 25% margin. Assume any power cables and wires have trivial mass.
ReachBot Perception Strategy	Two-stage with possible gripper-level force sensing. Near-field is defined as the distance of one-third of the boom length.

relates to the angle, distance, and reflectivity of the surface. We note that there are other types of LiDAR technologies such as focal plane array (Flash) LiDAR, frequency modulated continuous wave (FMCW) LiDAR. These have very long range (beyond 150 m), but are generally low spatial resolution at a distance. The low data density can be mitigated by mounting the LiDAR unit on a motorized tilt platform for sweeping samples. Another drawback of LiDAR is degraded performance in dusty or foggy conditions which may occur in the subsurface. However the major benefit is LiDAR does not need external illumination. Because we plan to operate in a 3D terrain environment, we are only interested in 3D LiDAR.

2D Cameras—Monocular cameras represent the scene as a 2D array of pixels, which can either be color or grayscale. It is possible to detect depth using structure from motion or other techniques, and planar images have been used in combination with LiDAR to estimate motion. For example, high-frame-rate event cameras report changes at the microsecond scale [32]. Monocular cameras also will require onboard illumination to function in a subterranean environment, which could introduce issues with shadows, brightness differences, specular reflections, and occlusions. This could make visual and visual-inertial mapping difficult downstream.

3D Cameras—Depth cameras such as RGB-D or stereo can produce 3D or depth data as well as traditional images. Stereo cameras work by extracting depth information from multiple monocular cameras that are arranged with known extrinsic/intrinsic parameters. RGB-D cameras, such as the Intel Realsense, provide both color and depth information. Active RGB-D cameras project patterns of structured infrared light into a scene and use the sensed deformation of the patterns of objects in the scene to accurately estimate depth, which is more robust to lack of proper illumination. Despite this, the IR light and thus depth measurements have degraded performance in brighter outdoor environments. More discussion on active 3D vision cameras can be found in [33].

Sonar—Sound navigation and ranging (SoNAR) sensors measure ToF of ultrasound waves. SoNAR trades off short-range precision with spatial accuracy, and has been found to fare better in humidity than LiDAR [34]. Like LiDAR, SoNAR does not require active illumination. There exists several commercially-available sonar sensors.

Radar—Radio detection and ranging (RADAR) is another active range sensing technology. As with SoNAR, RADAR does not require light or temperature gradients to operate, and system-on-chip (SoC) radars have low power draws. However, radars can be adversely affected by sensor noise, spatial resolution, and data corruption (e.g. multipath reflections) [35]. Millimeter-scale radar waves are also large enough to be

less affected by small airborne particulates, which can cause reflections with LiDAR; however, radar is not as common as camera vision on subsurface robots today [18].

Thermal—Thermal vision detects the magnitude of infrared radiation which can be output as a 2D heat signature image. Thermal sensing has previously been shown for ground granularity prediction in wheeled robot navigation [36]. However, the usefulness of thermal vision depends on differences in temperature; while on the surface, thermal transients are expected due to periodic illumination, in subsurface caves such gradients are often minimal. It is noted that thermal may be useful if there is water present, or if there is an opening in the ground, especially as thermal vision is not affected by dust degradation [22].

Sensor Evaluation Criteria

Trade studies require criteria to evaluate both effectiveness and performance, so we list the following criteria:

1. **Spatial Resolution.** As a requirement, we need enough spatial resolution to distinguish grasping site features. The smallest graspable surface would involve a pinch grasp, and we model this surface as a 50 mm diameter hemisphere as based on the ReachBot palm size. Therefore we require a spatial resolution of 25 mm^2 per measurement or better when near-field sensing (this can be obtained through multiple sensors or sensor fusion techniques if not outright). If the minimum resolution at the near-field sensing distance is achieved, the objective is to have high spatial resolution at a distance; the higher the spatial resolution the better the score. We may also weigh this score by sensor range to optimize for sensors with high resolution at mid to long ranges.
2. **Spatial Accuracy.** Accurate distance measurements are vital for precise navigation and manipulation. For this trade study we do not list a specific accuracy requirement but have this criteria as an objective: the more accurate the sensor, the higher the score.
3. **Range.** The detection range impacts ReachBot’s ability to detect distant obstacles or grasping sites, so range capabilities are required for the sensors. For a near-field sensor, we have defined near-field previously as being one-third of the total boom length, so we require sensing at least from 3.3 m for a 10 m-long boom. We assign a higher score if able to sense at a closer distance. For a far-field sensor, we require a minimum detection range from the one-third length to the full length of the boom. Given the lava tube environment dimensions (Table 1), we assign a higher score for more distance, though with no need beyond 20 m. To avoid blind spots in sensing range, there should be some switchover bandwidth built in when switching from far- to near-field sensing.
4. **Field of View.** This is an objective to maximize field of view; there is no minimum field of view required. Because

ReachBot must be able to map not only floors, but walls and ceilings, we assign a higher score for sensors with higher field of view. We note that some sensors may be mounted on mechanisms to increase their field of view, such as a motorized platform.

5. **Robustness to Darkness.** Sensors must withstand harsh planetary environments to ensure long-term reliability and minimize maintenance needs. Sensors are required to be able (or can be augmented) to operate in consistent total darkness.

6. **Robustness to Dust.** Sensors are required to be able (or can be augmented) to operate in dusty conditions.

7. **Power Efficiency.** Energy-efficient sensors help maximize mission duration and reduce the need for frequent recharging. Power efficiency is an objective not a requirement, so the more power efficient, the higher the score.

8. **Implementation Ease.** The ideal sensor would levy no constraints on the design of the rest of the system, are supported by the manufacturer and the scientific robotics community, and require no additional modifications to operate. Higher scores are given to sensors with recent and widespread heritage in subsurface robotics and are still supported.

9. **Lightness and Compactness.** As with any space application, minimization of mass and volume is essential. Higher scores are given to lightweight, compact sensors (objective) that fit within the ReachBot mass budget (requirement).

10. **Affordability.** This metric was included to favor options that could be inexpensively prototyped and tested. The more inexpensive and easy to obtain, the higher the score.

We note that there are many other evaluation criteria that could have been chosen, such as robustness to extreme temperatures, radiation resistance, or computation efficiency. The ultimate goal for this trade study is to use this analysis to inform a feasible perception system prototype; if ReachBot is selected for a space mission then a more exhaustive study can be done in the future to include space hardiness parameters. As a result, we assign a weight of 2 to performance-based criteria (Resolution, Accuracy, Range, Field of View, Robustness to Darkness, Robustness to Dust) and a weight of 1 to the space-worthiness criteria (Power Efficiency, Implementation Ease, Lightness and Compactness, Affordability).

5. SENSOR TRADE RESULTS

Given multiple range-sensing technologies and ReachBot-specific evaluation criteria, we now present the results of our trade study.

Sensor Modality Trades for ReachBot

To fully instrument a ReachBot for a lava tube mission, we conduct a trade to select the primary modalities for ReachBot and report these results in Table 2. More detail on the construction of this table is reported in the appendices.

First, we analyse the table for the best modality in far-field sensing (scored "High" in range) and find LiDAR to be the best sensor type across our desired characteristics for far-field sensing. This aligns with other subsurface robotics literature, which generally also have LiDAR-centric perception systems [18]. Because of its capabilities over long ranges, we choose LiDAR as the primary far-field sensing solution.

Since ReachBot must be able to see both the floor and ceiling, the LiDAR unit will be mounted on the body of ReachBot and may have additional supporting systems. For example, one supporting system pairs the LiDAR with an IMU on a spinning, tilted mount, similar to the CatPack pioneered by

CSIRO's Wildcat system [19]. This mount increases the field of view dramatically; a Velodyne VLP-16 LiDAR mounted on such a system provides 120° vertical field of view instead of the usual 30°, therefore allowing ReachBot to perceive the floor, walls, and ceiling of the lava tube at great distances though with added software and mechanical complexity. As another example, we may employ two LiDAR units, with one tilted for primarily ground-to-wall coverage in the forward direction, and the other for primarily wall-to-ceiling coverage in the forward direction.

For further redundancy and resilience to edge cases, the primary LiDAR modality can be complemented with other sensing. Based on the results of Table 2, we consider also pairing LiDAR with radar, which is able to cover long ranges and is also robust to dusty conditions in cases where LiDAR may fail. An example radar sensor is the Texas Instruments AWR1843 sensor, which has been previously used for robotics [35, 37]. However, we note that the integration of radar sensing is not as established as other sensing modalities because of the complexity of the corresponding sensor models and data, so more research must be done to tightly couple the two modalities.

For the near-field sensing (ranked "Low" or "Mid" in range), 3D cameras perform best. This sensor will be mounted at the distal end of the boom. An example of a 3D camera is the Intel Realsense D435i, which has seen widespread use in robotics. One additional benefit to having a RGB vision capability at the distal end of the boom is the ability to capture color images of geological features for scientific study. This will require onboard active illumination at the sensor itself for color images, and further analysis can be done on the illumination design.

Therefore, from a modality standpoint, a fully-instrumented ReachBot with a multimodal perception suite should consist of LiDAR and radar located in the body and a 3D camera located at the distal end of each boom. One possible ReachBot body system that fulfills these modalities would be two Velodyne VLP-16 pucks mounted at opposing 45° angles and forward- and rear-facing Texas Instrument AWR1843 System on Chip automotive-grade radar sensors (all together ≈1.7 kg).

Sensor Component Trade for a Prototype

In the end, we would like to build a physical prototype of the perception system. Towards this, in Table 3, we report the specific evaluations of several commercially-available sensors² for ReachBot based on the evaluation criteria. These sensors were chosen because they are either already in our possession, or are used previously in literature and purchaseable online. The full treatment with all parameters and details is included in the appendices.

For LiDAR-based far-field sensing, we currently possess a Velodyne VLP-16 unit, but would like to compare this unit against alternative LiDAR units that are purchaseable online, in case they perform better. Since we already have a Velodyne unit, in the trade we give "Affordability" full marks; because LiDAR units are quite costly we assign a weight of "2" for the "Affordability" metric. Since we want to be able to quickly prototype, we also assign a weight of "2" for the "Implementation Ease" metric. The results of this comparison is shown

²We note that in the case of the Apple iPhone 12 LiDAR, detailed technical information is not publicly available, so we use approximate values reported in literature [38].

Table 2. Modality Evaluation: The capabilities and basic sensor information of various sensor categories commonly used robotics applications as summarized in terms of ReachBot evaluation criteria. We prioritize performance-based criteria (Resolution, Accuracy, Field of View, Range, Robustness to Darkness, Robustness to Dust) by a weight of 2, and all others by a weight of 1.

Modality	Example Device	Resolution	Accuracy	Field of View	Range	Power Efficiency	Robustness to Darkness	Robustness to Dust	Implementation Ease	Lightness and Compactness	Affordability
LiDAR	Velodyne VLP-16	High	High	High	High	Low	High	Low	High	Low	Low
2D Camera	FLIR Firefly S	High	High	High	Low	Mid	Low	Low	High	Mid	High
3D Camera	IntelD435i	High	High	High	Low	Mid	High	Low	High	Mid	Mid
Radar	XM132	Mid	Mid	Mid	High	High	High	High	Mid	High	Mid
Sonar	MaxBotix MB1000	Mid	Mid	Mid	Mid	High	High	High	Mid	High	Mid
Thermal	FLIR Tau2	Mid	Mid	Mid	Mid	Mid	High	Mid	Low	Mid	Mid

Table 3. Sensors considered for building a ReachBot prototype, where each device is scored from 0 to 2 per criterion. The scores are multiplied by the respective weight and a weighted sum is produced. More details are in provided in the Appendix for the score margins.

Sensor Type	Device Name	Resolution	Accuracy	Field of View	Range	Robustness to Darkness	Robustness to Dust	Power Efficiency	Implementation Ease	Lightness and Compactness	Affordability	Weighted Sum
Far-field Sensing												
LiDAR Weights		2	2	2	2	2	2	1	1	1	2	
LiDAR	RSBPearl	2	2	2	1	2	1	1	1	1	0	23
LiDAR	Velodyne Puck (VLP-16)	1	2	1	2	2	1	1	2	1	2	26
LiDAR (ToF)	Cygbot Mini Lidar	1	2	0	0	2	1	2	0	2	2	20
LiDAR	iPhone 12	2	2	1	0	2	1	2	1	2	1	23
LiDAR	Ouster OS1-32	2	2	2	2	2	1	1	1	2	0	26
Near-field Sensing												
Weights		2	2	2	1	2	2	1	2	2	2	
Monocular RGB Camera	FLIR Firefly S	1	1	1	1	0	0	1	0	2	1	14
Active 3D (ToF, IR)	Intel D435i	2	2	1	1	1	0	1	2	1	2	24
Active 3D (ToF, IR)	Intel D455i	1	2	1	1	1	0	1	2	0	2	20
Active 3D	StereoLabs Zed2	2	2	2	2	1	0	1	1	1	1	23
Active 3D	OAK-D	1	2	1	1	1	0	1	1	1	1	18

using the existing Velodyne VLP-16 unit in our possession.

in the far-field sensing section of Table 3.

Based on the weighted scoring, the Velodyne VLP-16 and Ouster OS1-32 unit are both good options for ReachBot's primary LiDAR unit. The Ouster OS1-32 outperforms the Velodyne unit on both resolution and field of view, but costs over \$6000 to purchase online, which is quite prohibitive. Unless a unit is available for a cheap price, we will develop

For vision-based near-field sensing, we currently possess an Intel D455 RGB-D camera that was used in field tests [13], and an Intel D435i. We would like to compare them against alternative RGB-D cameras and investigate which option fares best given a better understanding of the sensing evaluation requirements for near-field sensing. The results are shown in near-field sensing section of Table 3.

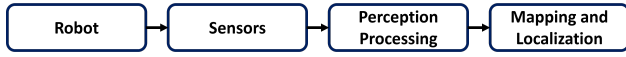


Figure 3. Basic flowchart of perception system. The majority of this trade study focused on defining hardware constraints and optimization objectives (hardware, sensors), but we also discuss different representation possibilities for ReachBot downstream in order to provide a full picture of the perception system.

Based on the weighted scoring, the Intel D435i and the Stereolabs Zed2 are both good options for ReachBot’s primary near-field sensing unit. The Intel D435i, as a commonplace sensor in robotics with many open-source libraries for realsense software, scored highest for implementation ease. Based on this trade study, we recommend using the Intel D435i for near-field sensing. However, the Zed2 has a wider field of view, a wider range, and is 100 g lighter than the Intel D435i, and presents a good second option.

The result of this trade study is a recommendation for the specific primary component for both far- and near-field sensing. Based on this analysis, we will use a Velodyne VLP-16 unit for far-field sensing and an Intel D435i for near-field sensing. We have also identified promising alternatives to both components should product cancellations or other external vendor delays occur.

6. GRASPING SITE REPRESENTATION ANALYSIS

As shown in Fig. 3, the goal of the perception system is to provide a map output (of the grasping sites) for the planner. We have thus far developed the primary and secondary modalities for ReachBot, and suggested specific sensor components for further prototyping. Now we will provide some analysis of the software architecture for ReachBot’s perception system, but leave specific recommendations to future work.

At a high level, the choice of map representation should provide compatible inputs for the planner. For identifying grasping site locations, a force-torque limit surface can be generated given known gripper parameters and macro rock geometry with conservative rock friction properties assumed. Macro rock geometry is perceived from the sensors discussed in the previous section, and can be parameterized (curvature, radius, centroid of location) and stored in the terrain map. The computation of a limit surface is somewhat time consuming (highly dependent on contact details of microspines on rock surfaces), but could be pre-computed offline for typical cases or learned from representative cases. This would likely be implemented as an additional layer when processing perceptual data to output to the planner.

Terrain representation types can generally be categorized as 2D, 2.5D, and 3D maps, and extensive surveys exist detailing more specific options for robotic exploration [1]. The choice of map type trades accuracy and resolution with computational efficiency and memory storage. Given that a lava tube is a highly unstructured outdoor environment, we focus only on analyzing 2.5D and 3D map representations for this trade study.

2.5D Maps

The most common 2.5D mapping method is an elevation map, where (x, y) locations are augmented with a height h of the surface. Naturally, elevation maps make sense for environments where heights can be computed, such as the floor of a mine shaft or any such space with a guaranteed ground floor. The ANYmal platform uses elevation maps for real-time surface reconstruction, called GridMap [39].

3D mapping

Pointclouds represent occupied points but are generally not used for real-time planning. OctoMap is a more efficient representation of occupancy probabilities, but using Octrees (a tree data structure) to divide a 3D space into octants [40]. OctoMaps allow for empty and unexplored spaces to be represented. Another representation is to use Truncated Signed Distance Functions (TSDF), which is a technique from computer graphics that measures the distance between each point in a point cloud and the surface of an object being represented [41]. Another representation can be a mesh which defines an object shape as a series of triangular meshes, which have highly descriptive capabilities at expense of computation cost [42].

Discussion and Suggested Criteria

As with any real robot system, we would like to keep memory and computation costs low. There are also some criteria that are specific for ReachBot’s tasks: being able to represent multiple scales of resolution, and being able to represent unstructured 3D environments. Although we leave this for a future trade study, we suggest a few usability criteria for map representations in confined spaces:

- Low memory usage
- Low computation overhead
- Multiple-scale environments (especially with respect to near- and far-field sensing)
- Multiple resolutions (especially with respect to near- and far-field sensing)

7. CONCLUSIONS

In this work, we analyze perception system design tradeoffs and develop the configuration of sensor modalities for a ReachBot mission to a martian lava tube. We also discussed overall perception strategy and different mapping representations for ReachBot. We find that a LiDAR-centric approach is the best far-field modality for a ReachBot mission; this also aligns with existing literature on LiDAR-based solutions, which have become increasingly robust to challenging environments and are common primary sensing modalities for subsurface robots. We also recommend a specific LiDAR sensor for prototyping, and find that supporting LiDAR with another complementary modality such as radar will make the system more robust to dusty conditions. Finally, we find that for near-field sensing, 3D vision such as RGB-D cameras perform best and we recommend a specific camera sensor for further development work.

Having identified leading COTS component candidates for the ReachBot perception system, our future work involves refining the implementation details. These include hardware testing and characterization, investigation into illumination approaches to support the near-field vision sensing, and further development of the grasp site representation. Future work for grasp site reconstruction could include investigation

into deep learning and neural radiance fields, or increasing robustness in even more adverse conditions such as the specular ice walls of the Martian poles or Europa!

APPENDICES

A. MODALITY ANALYSIS

Here are the cut-off ranges selected for the descriptions in Table 2.

- **Resolution:** We consider high resolution to be capable of returning 2MP or more. We define low resolution as only able to return 0.5MP or less.
- **Accuracy:** We consider high accuracy to be less than or equal to 2% error at nominal range, and low accuracy to be greater than 10% error at nominal range (as reported by the manufacturer).
- **Field of View:** We consider high field of view to be greater than 90° in either vertical or horizontal field of view without any additional support (i.e. special motorized mounts).
- **Range:** We consider greater than the nominal boom length of 10 m as high range. We consider less than 3 m as low range.
- **Power Efficiency:** We consider high power efficiency to be mW-level power draw, mid power efficiency to be on the order of 1 W power draw, and low power efficiency to be on the order of 10 W power draw.
- **Robustness to Darkness:** We consider high robustness to darkness if the sensor is invariant to illumination. We note that in the case of 3D cameras, the RGB portion of the camera is not illumination invariant, but the depth portion is. We consider low robustness to darkness if the sensor cannot produce useable data in darkness conditions.
- **Robustness to Dust:** We consider high robustness if the sensor is invariant to dust. We consider low robustness if dusty conditions causes substantial decrease in data quality.
- **Implementation Ease:** We consider high implementation ease if the technology has been used in many subsurface robots (such as those in the DARPA Subterranean Challenge) and existing literature. We consider low implementation ease if the technology has only been used in one or two subsurface robots or requires more research.
- **Lightness and Compactness:** We consider "High" to be under 10 grams (implementable on a chip); and "Low" to be over 500 grams (must be mounted).
- **Affordability:** We consider prices in the order of magnitude of 10 USD to be highly affordability, 100 USD to be mid affordability, and 1000 USD to be low affordability.

B. SENSOR ANALYSIS

In the following table, Table 4, we include the full technical details for the sensors considered in this trade study.

Table 4. Sensors Considered for ReachBot: Full values for LiDAR sensors.

Sensor Type	Device Name	Resolution	Accuracy	Field of View	Range	Robustness to Darkness	Robustness to Dust	Power Efficiency	Implementation Ease	Mass	Size	Affordability
Lidar	RSB Pearl	32 channel horizontal angular resolution 0.2°	±2 cm	360° x 90°	30 m	High	Low	13W	Low	920g	100mm x 111mm	\$3000-4000
Lidar	Velodyne Puck (VLP-16)	vertical angular resolution 0.4°	16 channel 0.1° ±3 cm	360° x 30°	100 m	High	Low	8W	High	830g	103mm x 72mm	\$4,000
Lidar (ToF)	Cybot Mini Lidar	horizontal angular resolution 0.4°	vertical angular resolution 0.4°	65°	50mm	High	Low	-	Low	28g	37.4*37.4*28mm	\$170
Lidar	iPhone 12	-	-	120°	5 m	High	Low	-	Low	164 g	146.7 x 71.5 x 7.4mm	\$999
Lidar	Ouster OS 1-32	32 channel 0.35°	± 1.5 cm	45° (± 22.5°)	120 m	High	Low	14 – 20 W	High	495g	87 mm x 74.2 mm	\$6,600
Monocular RGB Camera	FLIR Firefly S	1440 x 1080				Low	Low	2.2 W	Low	20 g	27 mm x 27 mm x 14.5 mm	\$234
Active 3D (ToF, IR)	Intel D435i	1920 × 1080	±2% at 2 m	87° × 58°	0.3 - 3m	High	Low	2W	High	260 g	90mm x 25 mm x 25 mm	\$334
Active 3D (ToF, IR)	Intel D455i	1280 × 800	±2% at 4 m	87° × 58°	.6 m to 6 m	High	Low	-	High	380 g	124 mm x 26 mm x 29 mm	\$419
Active 3D	StereoLabs Zed2	1920x2080		110° (H) x 70° (V) x 120° (D)	0.3 m to 20 m	High	Low	1.9W	Mid	166 g	175 x 30 x 33 mm	\$499
Active 3D	OAK-D	1280x800		89° x 80° x 55°	0.7m - 8m	High	Low			115 g	110x54.5x33mm	\$249
Radar	XM132	11.3° azimuth- x 45° elevation		75° x 20°	0.5-10 m	-	-	0.05 mW	Low	4 g	25 x 20 mm	\$20.00
Radar	TI AWR1843				12m	-	-		Low	-	10.4 mm x 10.4 mm	\$299

ACKNOWLEDGMENTS

Support for this work was provided by NASA under the Innovative Advanced Concepts program (NIAC) and by the Air Force under an STTR award with Altius Space Machines. Thank you to Stephanie Newdick and Tony Chen for providing feedback on this manuscript.

REFERENCES

- [1] S. Schneider, A. Bylard, T. G. Chen, P. Wang, M. Cutkosky, M. Lapôtre, and M. Pavone, "Reachbot: A small robot for large mobile manipulation tasks," in *2022 IEEE Aerospace Conference*. IEEE, 2022, pp. 1–12.
- [2] T. G. Chen, B. Miller, C. Winston, S. Schneider, A. Bylard, M. Pavone, and M. R. Cutkosky, "Reachbot: A small robot with exceptional reach for rough terrain," in *2022 International Conference on Robotics and Automation (ICRA)*. IEEE, 2022, pp. 4517–4523.
- [3] S. Newdick, T. G. Chen, B. Hockman, E. Schmerling, M. R. Cutkosky, and M. Pavone, "Designing reachbot: System design process with a case study of a martian lava tube mission," in *2023 IEEE Aerospace Conference*. IEEE, 2023, pp. 1–9.
- [4] S. Newdick, N. Ongole, T. G. Chen, E. Schmerling, M. R. Cutkosky, and M. Pavone, "Motion planning for a climbing robot with stochastic grasps," in *2023 IEEE International Conference on Robotics and Automation (ICRA)*. IEEE, 2023, pp. 11 838–11 844.
- [5] J. S. Roberts, P.-E. Giacomelli, Y. Gozlan, and J. Di, "A skeleton-based approach for rock crack detection towards a climbing robot application," *arXiv preprint arXiv:2309.05139*, 2023.
- [6] A. T. Asbeck, S. Kim, M. R. Cutkosky, W. R. Provancher, and M. Lanzetta, "Scaling hard vertical surfaces with compliant microspine arrays," *The International Journal of Robotics Research*, vol. 25, no. 12, pp. 1165–1179, 2006.
- [7] A. Parness, N. Abcouwer, C. Fuller, N. Wiltsie, J. Nash, and B. Kennedy, "Lemur 3: A limbed climbing robot for extreme terrain mobility in space," in *2017 IEEE international conference on robotics and automation (ICRA)*. IEEE, 2017, pp. 5467–5473.
- [8] S. Wang, H. Jiang, T. Myung Huh, D. Sun, W. Ruotolo, M. Miller, W. R. Roderick, H. S. Stuart, and M. R. Cutkosky, "Spinyhand: Contact load sharing for a human-scale climbing robot," *Journal of Mechanisms and Robotics*, vol. 11, no. 3, p. 031009, 2019.
- [9] S. B. Backus, R. Onishi, A. Bocklund, A. Berg, E. D. Contreras, and A. Parness, "Design and testing of the jpl-nautilus gripper for deep-ocean geological sampling," *Journal of Field Robotics*, vol. 37, no. 6, pp. 972–986, 2020.
- [10] M. T. Pope, C. W. Kimes, H. Jiang, E. W. Hawkes, M. A. Estrada, C. F. Kerst, W. R. Roderick, A. K. Han, D. L. Christensen, and M. R. Cutkosky, "A multimodal robot for perching and climbing on vertical outdoor surfaces," *IEEE Transactions on Robotics*, vol. 33, no. 1, pp. 38–48, 2016.
- [11] H. Jiang, S. Wang, and M. R. Cutkosky, "Stochastic models of compliant spine arrays for rough surface grasping," *The International Journal of Robotics Research*, vol. 37, no. 7, pp. 669–687, 2018.
- [12] A. T. Asbeck and M. R. Cutkosky, "Designing compliant spine mechanisms for climbing," *Journal of Mechanisms and Robotics*, 2012.
- [13] T. G. Chen, S. Newdick, J. Di, C. Bosio, N. Ongole, M. Lapôtre, M. Pavone, and M. R. Cutkosky, "Locomotion as manipulation: Grasp analysis for reachbot," p. under review, 2024.
- [14] K. Uckert, A. Parness, N. Chanover, E. J. Eshelman, N. Abcouwer, J. Nash, R. Detry, C. Fuller, D. Voelz, R. Hull *et al.*, "Investigating habitability with an integrated rock-climbing robot and astrobiology instrument suite," *Astrobiology*, vol. 20, no. 12, pp. 1427–1449, 2020.
- [15] T. H. Chung, V. Orekhov, and A. Maio, "Into the robotic depths: Analysis and insights from the darpa subterranean challenge," *Annual Review of Control, Robotics, and Autonomous Systems*, vol. 6, pp. 477–502, 2023.
- [16] M. Tranzatto, T. Miki, M. Dharmadhikari, L. Bernreiter, M. Kulkarni, F. Mascarich, O. Andersson, S. Khat-tak, M. Hutter, R. Siegwart *et al.*, "Cerberus in the darpa subterranean challenge," *Science Robotics*, vol. 7, no. 66, p. eabp9742, 2022.
- [17] A. Agha, K. Otsu, B. Morrell, D. D. Fan, R. Thakker, A. Santamaria-Navarro, S.-K. Kim, A. Bouman, X. Lei, J. Edlund *et al.*, "Nebula: Quest for robotic autonomy in challenging environments; team costar at the darpa subterranean challenge," *arXiv preprint arXiv:2103.11470*, 2021.
- [18] K. Ebadi, L. Bernreiter, H. Biggie, G. Catt, Y. Chang, A. Chatterjee, C. E. Denniston, S.-P. Deschênes, K. Harlow, S. Khattak *et al.*, "Present and future of slam in extreme underground environments," *arXiv preprint arXiv:2208.01787*, 2022.
- [19] N. Hudson, F. Talbot, M. Cox, J. Williams, T. Hines, A. Pitt, B. Wood, D. Frousheger, K. L. Surdo, T. Molnar *et al.*, "Heterogeneous ground and air platforms, homogeneous sensing: Team csiro data61's approach to the darpa subterranean challenge," *arXiv preprint arXiv:2104.09053*, 2021.
- [20] H. Azpúrúa, M. Saboia, G. M. Freitas, L. Clark, A.-a. Agha-mohammadi, G. Pessin, M. F. Campos, and D. G. Macharet, "A survey on the autonomous exploration of confined subterranean spaces: Perspectives from real-world and industrial robotic deployments," *Robotics and Autonomous Systems*, vol. 160, p. 104304, 2023.
- [21] T. Miki, J. Lee, J. Hwangbo, L. Wellhausen, V. Koltun, and M. Hutter, "Learning robust perceptive locomotion for quadrupedal robots in the wild," *Science Robotics*, vol. 7, no. 62, p. eabk2822, 2022.
- [22] M. Dharmadhikari, H. Nguyen, F. Mascarich, N. Khedekar, and K. Alexis, "Autonomous cave exploration using aerial robots," in *2021 International Conference on Unmanned Aircraft Systems (ICUAS)*. IEEE, 2021, pp. 942–949.
- [23] J. K. Ziemer, R. R. Wessen, and P. V. Johnson, "Exploring the science trade space with the jpl innovation foundry a-team," *Concurrent Engineering*, vol. 26, no. 1, pp. 22–32, 2018.
- [24] Quiñones, Sara Cuevas and Lapôtre, Mathieu (2023), Exploring Caves and Cliffs on Mars: Notional Mission Concepts Enabled by ReachBot, Abstract (P33B-04) presented at AGU23, 11-15 Dec.
- [25] E. National Academies of Sciences and

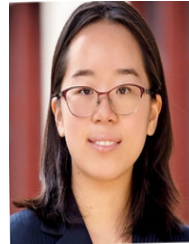
Medicine, *Origins, Worlds, and Life: A Decadal Strategy for Planetary Science and Astrobiology 2023-2032*. Washington, DC: The National Academies Press, 2023. [Online]. Available: <https://nap.nationalacademies.org/catalog/26522/origins-worlds-and-life-a-decadal-strategy-for-planetary-science>

- [26] F. Sauro, R. Pozzobon, M. Massironi, P. De Berardinis, T. Santagata, and J. De Waele, "Lava tubes on earth, moon and mars: A review on their size and morphology revealed by comparative planetology," *Earth-Science Reviews*, vol. 209, 2020.
- [27] J. Block, M. Straubel, and M. Wiedemann, "Ultralight deployable booms for solar sails and other large gossamer structures in space," *Acta astronautica*, vol. 68, no. 7-8, pp. 984–992, 2011.
- [28] C. Sickinger, L. Herbeck, and E. Breitbach, "Structural engineering on deployable cfrp booms for a solar propelled sailcraft," *Acta Astronautica*, vol. 58, no. 4, pp. 185–196, 2006.
- [29] F. Sauro, R. Pozzobon, M. Massironi, P. De Berardinis, T. Santagata, and J. De Waele, "Lava tubes on earth, moon and mars: A review on their size and morphology revealed by comparative planetology," *Earth-Science Reviews*, p. 103288, 2020.
- [30] U. Wong, A. Morris, C. Lea, J. Lee, C. Whittaker, B. Garney, and R. Whittaker, "Comparative evaluation of range sensing technologies for underground void modeling," in *2011 IEEE/RSJ International Conference on Intelligent Robots and Systems*. IEEE, 2011, pp. 3816–3823.
- [31] M. Leingartner, J. Maurer, A. Ferrein, and G. Steinbauer, "Evaluation of sensors and mapping approaches for disasters in tunnels," *Journal of field robotics*, vol. 33, no. 8, pp. 1037–1057, 2016.
- [32] G. Gallego, T. Delbrück, G. Orchard, C. Bartolozzi, B. Taba, A. Censi, S. Leutenegger, A. J. Davison, J. Conradt, K. Daniilidis *et al.*, "Event-based vision: A survey," *IEEE transactions on pattern analysis and machine intelligence*, vol. 44, no. 1, pp. 154–180, 2020.
- [33] R. Horaud, M. Hansard, G. Evangelidis, and C. M  nier, "An overview of depth cameras and range scanners based on time-of-flight technologies," *Machine vision and applications*, vol. 27, no. 7, pp. 1005–1020, 2016.
- [34] D. Silver, D. Bradley, and S. Thayer, "Scan matching for flooded subterranean voids," in *IEEE Conference on Robotics, Automation and Mechatronics, 2004.*, vol. 1. IEEE, 2004, pp. 422–427.
- [35] A. Kramer, C. Stahoviak, A. Santamaria-Navarro, A.-A. Agha-Mohammadi, and C. Heckman, "Radar-inertial ego-velocity estimation for visually degraded environments," in *2020 IEEE International Conference on Robotics and Automation (ICRA)*. IEEE, 2020, pp. 5739–5746.
- [36] C. Cunningham, I. A. Nesnas, and W. L. Whittaker, "Improving slip prediction on mars using thermal inertia measurements," *Autonomous Robots*, vol. 43, pp. 503–521, 2019.
- [37] A. Kramer, K. Harlow, C. Williams, and C. Heckman, "Coloradar: The direct 3d millimeter wave radar dataset," *The International Journal of Robotics Research*, vol. 41, no. 4, pp. 351–360, 2022.
- [38] G. Luetzenburg, A. Kroon, and A. A. Bj  rk, "Evalua-

tion of the apple iphone 12 pro lidar for an application in geosciences," *Scientific reports*, vol. 11, no. 1, p. 22221, 2021.

- [39] P. Fankhauser and M. Hutter, "Anymal: a unique quadruped robot conquering harsh environments," *Research Features*, no. 126, pp. 54–57, 2018.
- [40] D. Meagher, "Geometric modeling using octree encoding," *Computer graphics and image processing*, vol. 19, no. 2, pp. 129–147, 1982.
- [41] H. Oleynikova, Z. Taylor, M. Fehr, R. Siegwart, and J. Nieto, "Voxblox: Incremental 3d euclidean signed distance fields for on-board mav planning," in *2017 IEEE/RSJ International Conference on Intelligent Robots and Systems (IROS)*. IEEE, 2017, pp. 1366–1373.
- [42] M. Himmelsbach, F. V. Hundelshausen, and H.-J. Wuensche, "Fast segmentation of 3d point clouds for ground vehicles," in *2010 IEEE Intelligent Vehicles Symposium*. IEEE, 2010, pp. 560–565.

BIOGRAPHY



Julia Di is a Ph.D. candidate in the Biomimetic and Dexterous Manipulation Laboratory and was a NASA Space Technology Graduate Research Fellow with the NASA Ames Research Center Intelligent Robotics Group and NASA Jet Propulsion Laboratory. She received a B.S. degree in electrical engineering from Columbia University in 2018. Her research interests are vision-based tactile sensing and perception for robotic systems. Her goal in life is to explore the intersections of art and social good with technology.